Supporting Information

1D Aligned, *n-p* and *n-n* type ZnO Heterojunction Nanofibers for NO_2 Sensors: Exploration of Conduction Mechanism using *In-situ* Impedance Spectroscopy

*Ramakrishnan Vishnuraj[1], Mahaboobbatcha Aleem[1], Keerthi G Nair,[1] and Biji Pullithadathil[1]**

[1]Nanosensor laboratory, PSG Institute of Advanced Studies, Coimbatore – 641 004. India

*Corresponding author Email: bijuja123@yahoo.co.in; pbm@psgias.ac.in

1. Characterization Techniques:

The XRD patterns were acquired using Power X-ray diffractometer (Rigaku ULTIMA IV, Japan) using Cu Kα radiation of wavelength 1.5418 Å at a scanning rate of 0.02°/sec in the 2θ range of 20– 80°. Micro Raman spectra (Witech, 300 Alpha, Germany) of core-shell aligned *n*-ZnO/*p*-Bi_2O_3 and *n*-ZnO/*n*-In_2O_3 heterojunction nanofibers were obtained using λ = 532 nm as an excitation light source with 1800 g/mm gratings. The structure and morphology of the aligned *n*-ZnO/*p*-Bi_2O_3 and *n*-ZnO/*n*-In_2O_3 heterojunction nanofibers were examined using High-Resolution Transmission Electron Microscopy (JEOL JEM-2010, Japan) and Scanning Electron Microscopy (ZEISS EVO 18, US), with in-built energy-dispersive X-ray spectrometer (Oxford Instruments, INCA, UK). UV-DRS absorption spectra were acquired using JASCO UV (V-750) spectrophotometer. X-ray photoelectron spectroscopy (XPS) measurements were performed on a Phoibos 100 MCD Energy Analyser using monochromatized Al Kα excitation to analyze the elemental and chemical states of the materials. Brunauer-Emmett-Teller (BET) surface area analysis of samples was estimated by nitrogen adsorption-desorption isotherm (BELSORP-MAX, MicrotracBEL Corp, Japan).

2. Evaluation of gas sensor sensing properties:

The sensor device fabricated as inter-digitated array (IDA) electrode made of Au (~100 nm) with an inter finger gap of 80 µm using planar DC magnetron sputtering on alumina substrates. Aligned, *n*-ZnO/*p*-Bi_2O_3 and *n*-ZnO/*n*-In_2O_3 heterojunction nanofibers were directly spun on

to the IDA transducer electrodes using parallel plate collector and thermal treated at 550°C. The sensing properties of these materials were assessed using a custom-built gas sensor test station consisting of a stainless-steel double-walled test chamber equipped with temperature-controlled hot stage (Eurotherm, 2420, U.K.), sensor holder, MFC controllers (Alicat, USA) and the Agilent digital multimeter (34401A, USA) for data acquisition connected to a PC interfaced with Labview. High pure N_2 gas was used as the carrier gas for NO_2 for specific concentration and the pressure was constantly maintained at 300sccm. Baratron 722B Absolute Capacitance Manometer (MKS Instruments, Singapore) was used to regulate the chamber pressure**.**

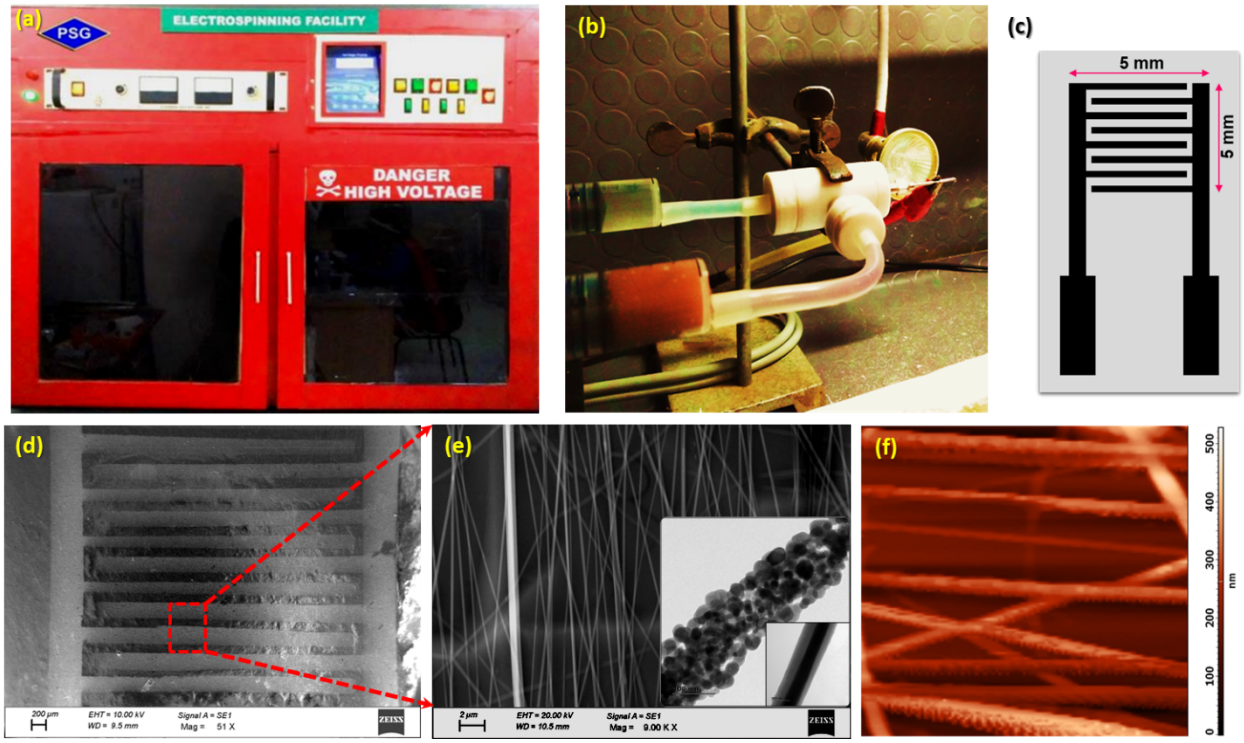

Figure S1 (a) Photograph of home-built Electrospinning unit (b) Photographs of the fabricated co-axial spinneret components fixed in the independent dual syringe pump (c) design of IDA electrode (d-e) SEM image of electrospun aligned nanofibers deposited on Au sputtered IDA electrode and (f) AFM image of annealed heterojunction nanofibers.

3. Electrospinning of ZnO nanofibers:

In this typical procedure, 8 wt% of PVA was dissolved in 29 mL of ultrapure water (Millipore Academic, Resistivity, 18.2 MΩ.cm) and kept for stirring. After formation of viscous solution 0.8 g of Zinc acetate was added slowly until the homogeneity appears. Then

the solution was finally stirred for 3 hours after the addition of 1 mL ethanol. A clear solution thus obtained was then subjected to electrospinning at a voltage, 25 kV with a feed rate of 0.2 mL/h. Thus, obtained ZnO/PVA nanofibers were annealed in a tubular furnace at 550°C for 3 hours to obtain crystalline ZnO nanofibers.

4. Optical Band gap calculation using UV–visible diffuses reflectance spectroscopy (DRS):

The band gap energy of the samples was measured by the extrapolation of the linear portion of the graph between the modified Kubelka-Munk function $[F(R)*h\nu]^2$ versus photon energy ($h\nu$) shown in the inset **Figure S2(b)**.

$$F_{KM} = \frac{(1-R)^2}{2R} \qquad (1)$$

The band gaps of the pristine ZnO, *n*-ZnO/*p*-Bi_2O_3 and *n*-ZnO/*n*-In_2O_3 heterojunction nanofibers were calculated to be 3.27, 3.14 and 3.20 eV respectively. The considerable change observed in the band gaps is due to the interfacial electron transfer between ZnO and respective *p*-Bi_2O_3 / *n*-In_2O_3 nanoclusters as shell layer.

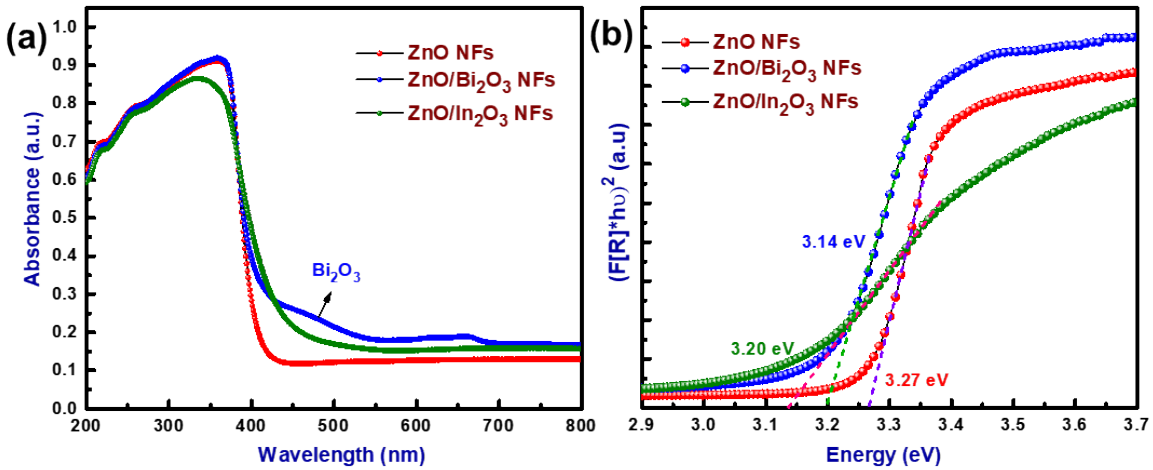

Figure S2(a) UV–Vis DRS spectra of pristine ZnO, *n*-ZnO/*p*-Bi_2O_3 and *n*-ZnO/*n*-In_2O_3 heterojunction nanofibers. (b) Kubelka-Munk function versus energy plots.

5. BET analysis:

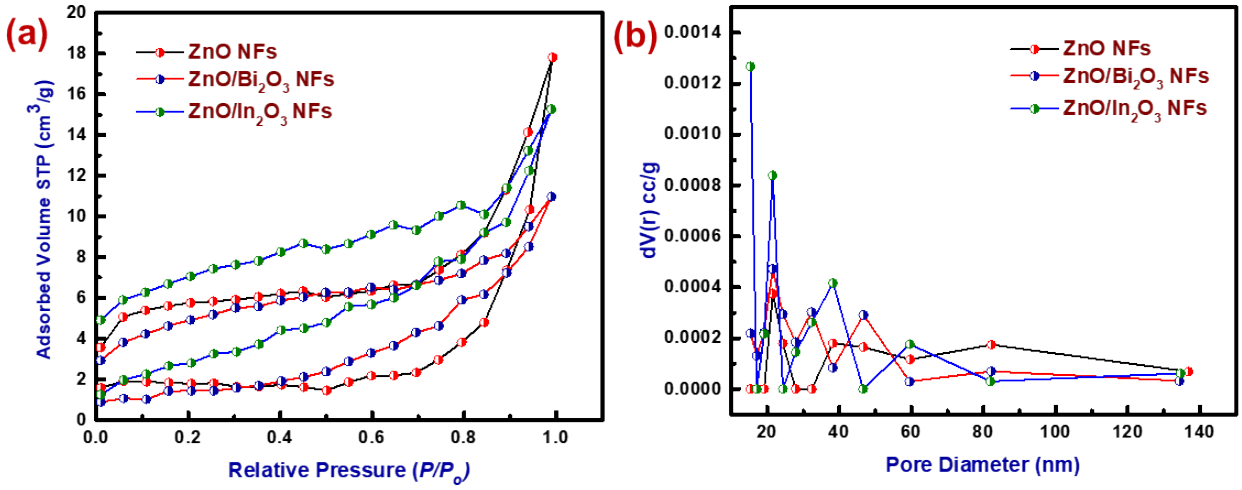

Figure S3 (a) Typical nitrogen adsorption–desorption isotherms of porous ZnO, *n*-ZnO/*p*-Bi_2O_3 and *n*-ZnO/*n*-In_2O_3 heterojunction nanofibers and (b) corresponding pore size distribution

Table S1. Parameters estimated from BET analysis of porous ZnO, *n*-ZnO/*p*-Bi_2O_3 and *n*-ZnO/*n*-In_2O_3 heterojunction nanofibers:

Materials	Surface area (m^2/g)	Pore volume (cm^3/g)	Pore size (nm)
ZnO nanofibers	5.695	6.6324	2.1547
ZnO/Bi_2O_3 heterojunction nanofibers	7.302	2.8475	2.0511
ZnO/In_2O_3 heterojunction nanofibers	16.012	3.5247	1.5355

Table: S2 Comparison of NO_2 gas sensing results:

Conc. of NO_2 (ppm)	ZnO nanofibers		ZnO/Bi_2O_3 nanofibers		ZnO/In_2O_3 nanofibers	
	$S_{Response}$%	$T_{Response}$(s)	$S_{Response}$%	$T_{Response}$(s)	$S_{Response}$%	$T_{Response}$(s)
0.5	31	5	365	8.0	843	5.6
1	82	5	820	7.8	1243	4.6
1.5	193	7	1210	6.0	1538	5.2
2	407	9	1927	5.0	1609	4.6
2.5	479	9	2551	5.3	2164	3.4
3	548	10	2732	5.2	2512	4.8

6. Cross Selectivity Studies:

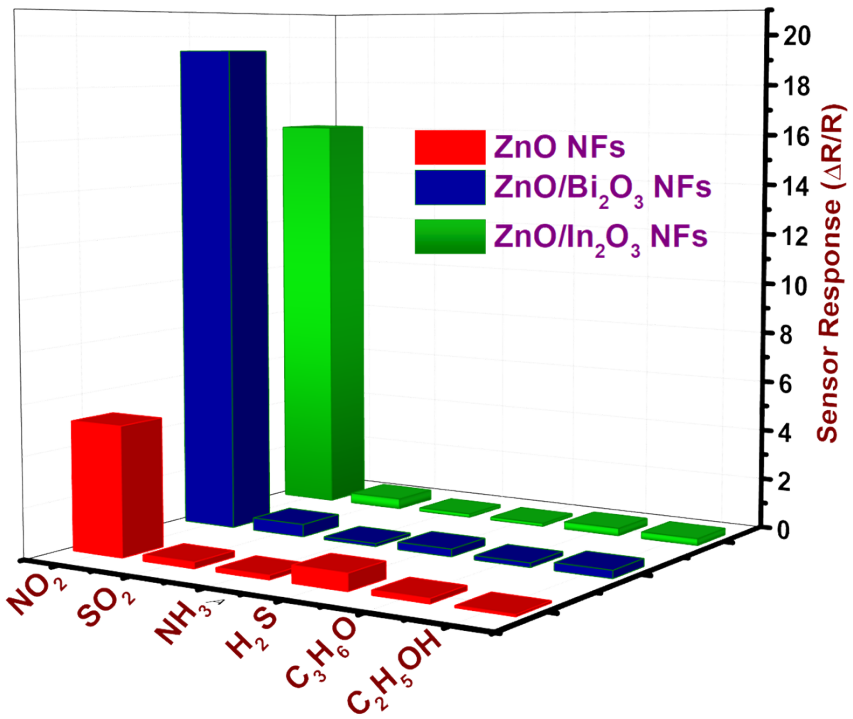

Figure S4 Cross selectivity studies of pristine ZnO nanofibers, aligned *n*-ZnO/*p*-Bi_2O_3 and *n*-ZnO/*n*-In_2O_3 heterojunction nanofibers.

7. Relative Humidity Interference Studies:

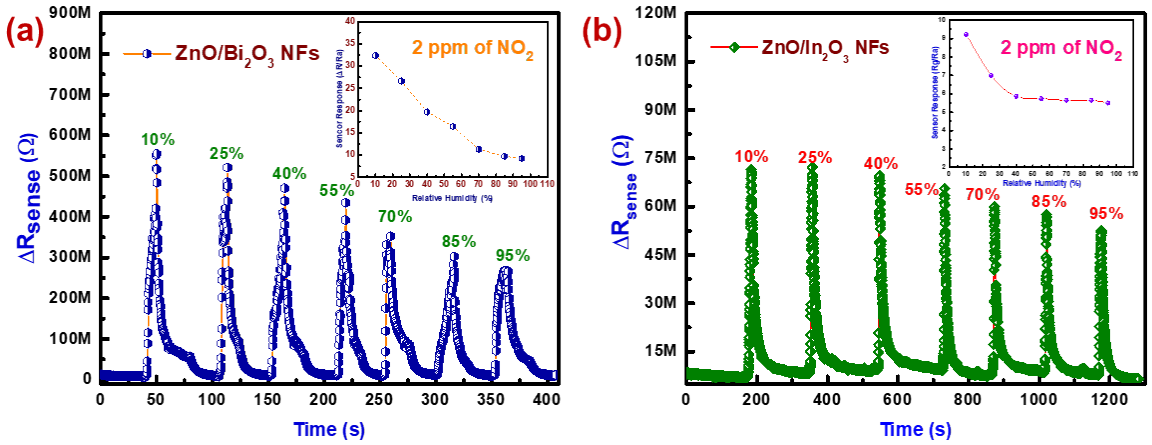

Figure S5. Relative humidity interference studies of (a) aligned *n*-ZnO/*p*-Bi_2O_3 heterojunction nanofibers and (b) aligned *n*-ZnO/*n*-In_2O_3 heterojunction nanofibers.

8. Repeatability and Stability:

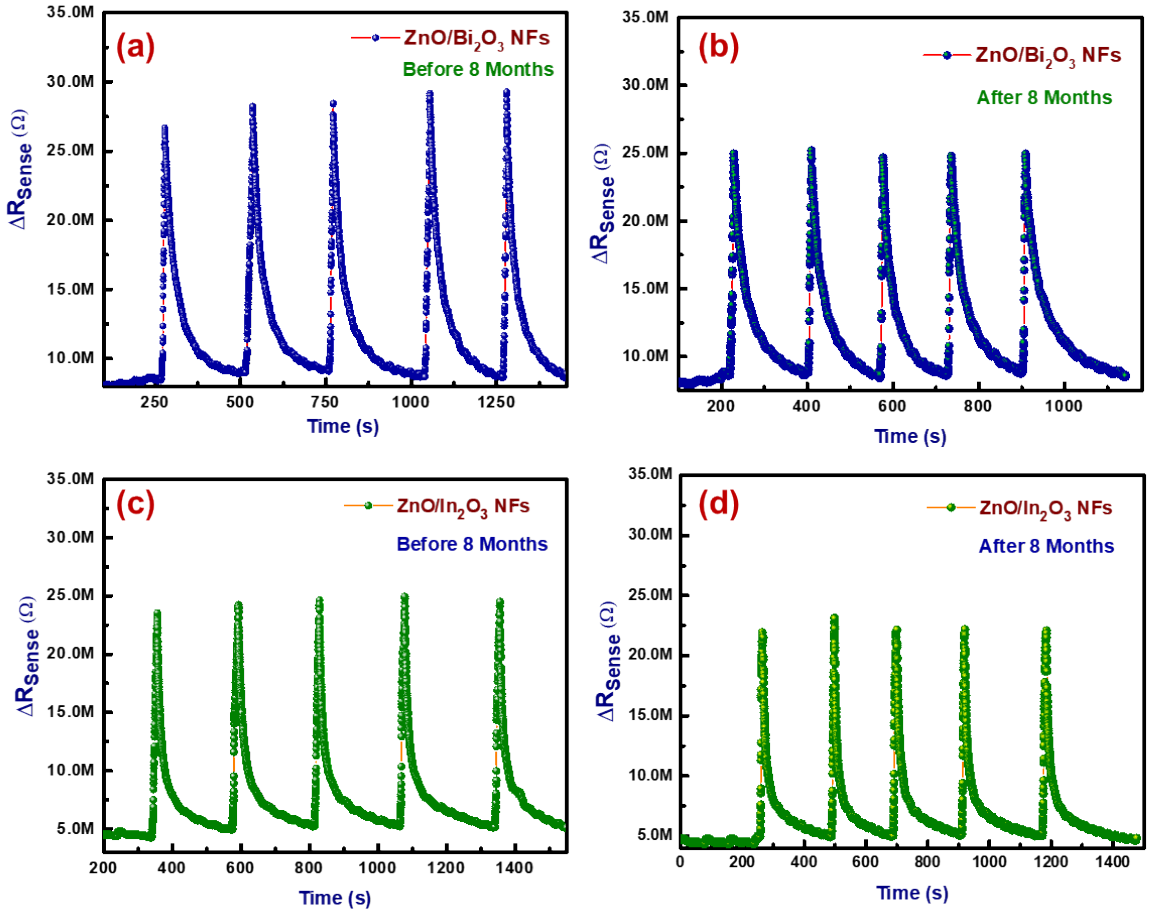

Figure S6. Repeatability and Stability studies of aligned *n*-ZnO/*p*-Bi_2O_3 heterojunction nanofibers (a) before 10 months and (b) after 10 months and aligned *n*-ZnO/*n*-In_2O_3 heterojunction nanofibers (c) before 10 months and (d) after 10 months.

9. AC-impedance Spectroscopic analysis:

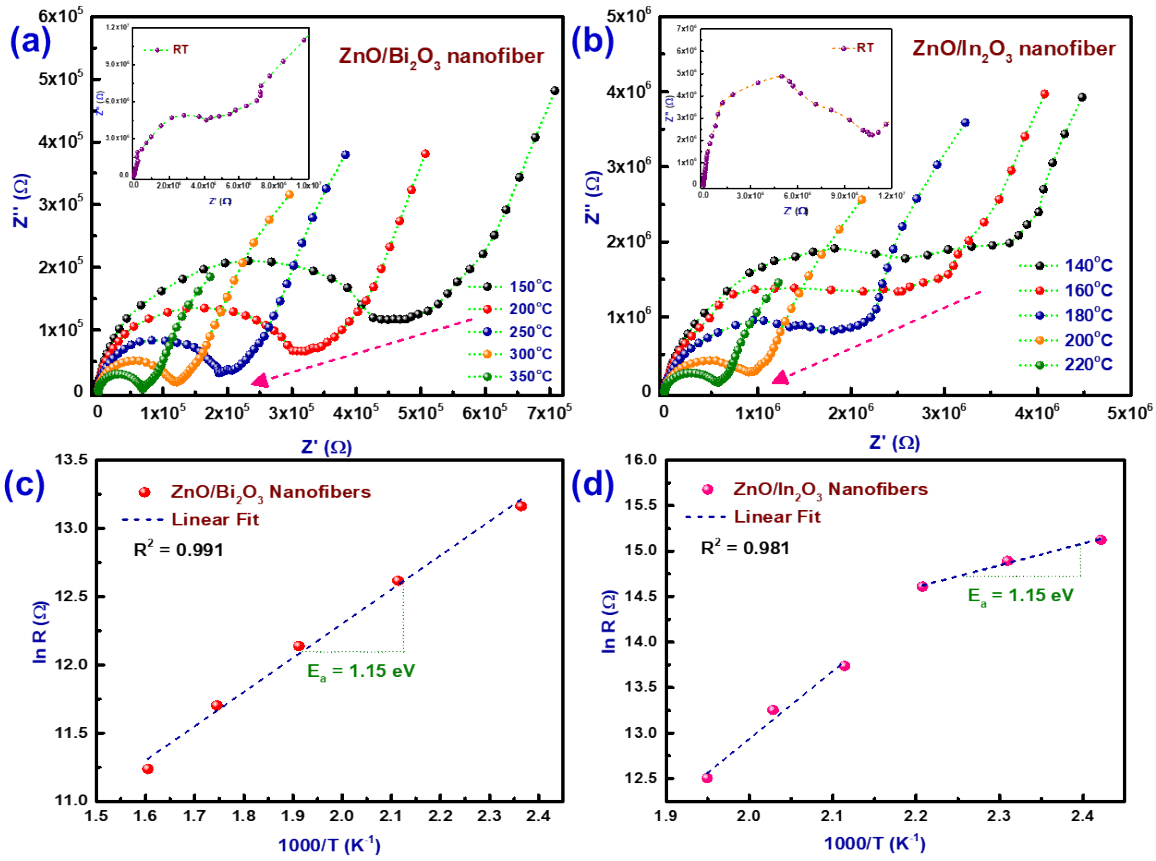

Figure S7 (a-b) Nyquist plot of the complex impedance at different temperatures for *n*-ZnO/*p*-Bi_2O_3 and *n*-ZnO/*n*-In_2O_3 heterojunction nanofibers, (c-d) Arrhenius plot of *n*-ZnO/*p*-Bi_2O_3 and *n*-ZnO/*n*-In_2O_3 heterojunction nanofibers.

Conditions	*n*-ZnO/*p*-Bi_2O_3 heterojunction NFs				*n*-ZnO/*n*-In_2O_3 heterojunction NFs			
	Z_0 (Ω)	Z_G(Ω)	Z_{GB}(Ω)	C_b (nF)	Z_0(Ω)	Z_G(Ω)	Z_{GB}(Ω)	C_b (nF)

Room Temperature	89.78	9.725e6	63.72e6	8.73	6.766	9.748e6	292.7	8.91
Operating temperature	24.69	141e3	254e3	8.69	34.89	344 e3	536 e3	8.89
0.5 ppm NO_2	25.76	196	116e3	7.10	102.9	450	656 e3	6.47
2 ppm NO_2	106.2	201e3	252e3	6.83	69.1	229e3	2.702e6	5.38

Table: S3 Fitted parameters attained for ZnO/Bi_2O_3 and ZnO/In_2O_3 HNFs:

Table: S4 Calculated parameters from the impedance analysis:

Conditions	Carrier Density (n_s) 10^{19} cm^{-2}		Depletion Width (nm)	
	n-ZnO/*p*-Bi_2O_3	*n*-ZnO/*n*-In_2O_3	*n*-ZnO/*p*-Bi_2O_3	*n*-ZnO/*n*-In_2O_3
Room Temperature	1.64	1.51	2.15	2.11
Operating temperature	1.63	1.44	2.16	2.12
0.5 ppm NO_2	1.08	0.77	2.64	2.89
2 ppm NO_2	0.98	0.53	2.76	3.48